ISBN: 978-3-95450-265-3 doi:10.18429/JACoW-SAP2023-TUPB033

HEATING ESTIMATION OF UNDULATOR VACUUM CHAMBER AT S^{3}FEL

Huaiqian Yi[1], Xiaofan Wang[1*], Weiqing Zhang[1,2†], Xueming Yang[1,2,3]
[1]Institute of Advanced Science Facilities, Shenzhen 518107, China
[2]Dalian Institute of Chemical Physics, Dalian 116023, China
[3]Southern University of Science and Technology, Shenzhen 518055, China

Abstract

Heating of the vacuum chambers are unavoidable when electron beams pass through the chamber channels at relativistic speeds. In the undulator vacuum chambers, such effects might lead to temperature increase of the magnets and eventually cause degradations in the FEL lasing process. Thus, in this paper, the heating of the undulator vacuum chambers at Shenzhen superconducting soft x-ray free-electron laser due to wake field effects and spontaneous synchrotron radiation are estimated using an analytical approach. For the wake field effects, the contribution from finite conductivity of the vacuum chamber material and from the inner surface roughness are considered. An electron beam profile from a start-to-end simulation is used to calculate the total wake field and the induced heat. For the synchrotron radiation, a simple analytical expression is used.

INTRODUCTION

At Shenzhen superconducting soft x-ray free-electron laser (S^{3}FEL) [1], electron beams from the injector system are accelerated in a single superconducting linac and transported to the undulator lines through the beam distribution system (BDS). At the end of the BDS, the typical electron beam parameters are given in Table 1. The maximum designed repetition rate of the electron bunches is 1MHz.

Table 1: Electron Beam Parameters

Beam Parameters	Value	Unit
Electron Energy	2.5	GeV
Slice Energy Spread	190	keV
Electron Bunch Charge	100	pC
Slice Emittance	0.5	mm·mrad
Rms Bunch Length	25	μm

When electron beams pass the vacuum chambers of the beam lines, heat will be deposited in the chamber walls due to electrons losing energy when interacting with their own wake fields.

The heating problems may become prominent for vacuum chambers in the undulators since the chamber transverse dimensions are small compared to other parts along the beam lines, and the wake filed effects are stronger. In addition, spontaneous synchrotron radiation is generated and absorbed by the chamber walls.

The vacuum chambers within the undulators at S^{3}FEL are made of extruded aluminium with an elliptical cross-section, as shown in Fig. 1. The full height and width of the chamber cavity are 6 mm and 15 mm, respectively. The two circular holes adjacent to the chamber are for the water-cooling system, while the two outermost holes are space designed for correction coils.

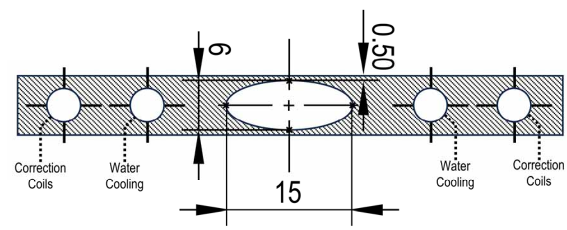

Figure 1: Cross-section of the vacuum chamber geometry.

If excessive heat in the vacuum chambers is not removed efficiently by the cooling system, the temperature gradient within the permanent magnet blocks will be affected and the magnetic field distributions and undulator K values will be modified. This will result in a negative impact on the FEL lasing process.

Under such considerations, the heat load projected on the vacuum chambers by the two heat sources mentioned above is estimated analytically in this paper. The results will serve as supplementary information to aid the design of the cooling system.

WAKE FIELD EFFECTS

The wake fields due to wall resistivity and the roughness of the inner surface of the vacuum chamber are considered in this work. Wake fields generated by single or periodic structures or other effects are ignored. A simplified approach is taken in the current calculations, where the longitudinal distributions of the electron beams is assumed to be unchanged as they travel down the undulator lines.

Calculation of the Wake Fields

The analytical approach first involves the calculation of resistive wall and roughness induced surface impedance and thereafter the longitudinal beam impedance Z. The latter depends on the cross-section shape of the vacuum chamber, and in this work, both round and flat plate

* wangxf@mail.iasf.ac.cn
† weiqingzhang@dicp.ac.cn

ISBN: 978-3-95450-265-3 doi:10.18429/JACoW-SAP2023-TUPB033

approximation of the chamber cross-section is assumed. The analytical expressions for coupling of the impedances due to resistance and wall roughness for round and flat geometries derived in [2] is used. An appropriate analytical model for elliptical shaped chamber is not yet available, but numerical calculations have shown that the beam impedances computed for elliptical cross-section shapes are very similar to those calculated using a flat plate model [3].

The resistive wall surface impedance, denoted as ζ_{rw}, is given by [2]:

$$\zeta_{rw}(k) = (1-i)\sqrt{\frac{k(1-ikc\tau_c)}{2Z_0\sigma_c}}, \tag{1}$$

where k is the wavenumber of the Fourier transform of the wake field, $Z_0 = 377\ \Omega$ is the impedance of vacuum, σ_c is and τ_c are the dc conductivity and the relaxation time of the metallic walls. The surface impedance due to roughness, denoted by ζ_{rs}, is given as [4]:

$$\zeta_{rs}(k) = \frac{1}{4}kh^2\kappa^{\frac{3}{2}}\left(\frac{\sqrt{2k+\kappa} - i\sqrt{2k-\kappa}}{\sqrt{4k^2-\kappa^2}}\right). \tag{2}$$

The roughness model assumes sinusoidal corrugation of the round pipes or of the flat plate model where the radius (or the half height of flat plate) r vary according to $r = a - h \cdot cos(\kappa z)$. For the model to be valid it is required that the period ($\lambda_{ro} = 2\pi/\kappa$) and the amplitude of the corrugation is small compared to the radius, i.e., $\kappa a \gg 2\pi$ and $h \ll a$, and that the corrugation is shallow ($h \ll 2\pi/\kappa$). The impedances given in Eq. (1) and Eq. (2) are defined for $k \geq 0$. For $k < 0$, the complex conjugate should be taken, i.e., $\zeta(-k) = \zeta^*(k)$ [5].

For a round vacuum chamber, the coupled beam impedance contains the contribution from both ζ_{rw} and ζ_{rs}, and is given by [2, 6]:

$$Z_r(k) = \frac{Z0}{2\pi a}\left(\frac{1}{\zeta_{rw}(k) + \zeta_{ro}(k)} - \frac{ika}{2}\right)^{-1}, \tag{3}$$

while for the flat plate model, the coupled beam impedance is [2, 7]:

$$Z_{fp}(k) = \frac{Z0}{2\pi a}\cdot$$

$$\int_{-\infty}^{\infty} sech(q)\left(\frac{cosh(q)}{\zeta_{rw}(k) + \zeta_{ro}(k)} - \frac{ika}{q}sinh(q)\right)^{-1} dq, \tag{4}$$

where q is the frequency component of another Fourier transform.

With the beam impedance known, the wake field of a single electron may be calculated with the inverse Fourier transform:

$$W_\delta(s) = \frac{c}{2\pi}\int_{-\infty}^{\infty} Z_{tot}(k)e^{-iks}dk\,, \tag{5}$$

where s is the distance behind the electron that invoked the wake field. Considering an electron beam that has a certain longitudinal distribution $f(s)$ (with unit C/m), the wake field along the beam longitudinal position can be calculated with the convolution:

$$W_f(s) = -\int_0^{\infty} W_\delta(s')f(s-s')ds'\,. \tag{6}$$

Using a typical electron beam longitudinal profile that is obtained from start-to-end simulation, the total wake field is computed according to Eq. (1-6). The integrations presented in these equations are performed numerically by selecting sufficiently small integration steps. As given in Fig. 1, the chamber radius or half height a is set to 3 mm. The aluminium conductivity and relaxation time are taken to be $\sigma_c = 3.5 \times 10^7 \Omega^{-1}\mathrm{m}^{-1}$ and $\tau_c = 8$ fs, respectively.

While the resistivity induced wake is well determined by the geometry and material of the chamber, the parameters for the roughness wake is uncertain due to the manufacturing process. However, practical experience suggested that the roughness surface thickness local maxima and minima difference is around 200 nm, which corresponds to $h = 100$ nm. The determination of the roughness oscillation wavelength is even more ambiguous, thus, the wake fields generated along the beam with different h and λ_{ro} values for the flat plate pipe model are compared in Fig. 2.

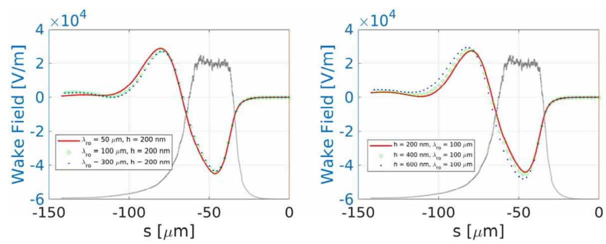

Figure 2 Electron beam wake field calculated using the round pipe model, for different surface roughness amplitudes (left) and for different corrugation wavelength (right). The beam profile is shown in grey.

It can be seen that variations of the roughness parameters have very limited influences on the total wake field and, consequently, on the amount of heat generated. Similar behaviours are also observed for the round model. Hence, the values for the roughness parameters are used in calculations hereafter are $h = 200$ nm and $\lambda_{ro} = 100$ µm.

Based on these parameters, a comparison of the wake field calculated with round and flat model, and their corresponding effects on the electron beam longitudinal energy distribution, after passing 10 undulator segments (i.e., travelling a distance of ~40 meters), are shown in Fig. 3. In calculation of the beam energy change, the longitudinal distribution of the beam is assumed to stay unchanged. The advantage of choosing longer horizontal width of the vacuum chamber is thus clear since the flat plate model predicts lower influence on the beam energy as compared to the round pipe model.

ISBN: 978-3-95450-265-3 doi:10.18429/JACoW-SAP2023-TUPB033

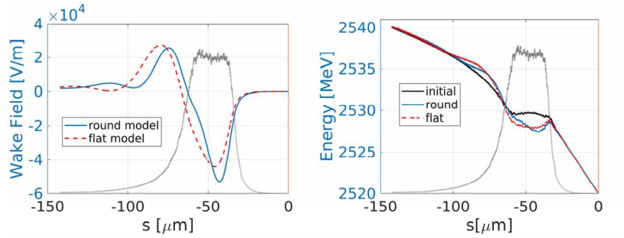

Figure 3 Wake field calculated using the round pipe model and flat plate model (left), and their corresponding influences on the electron beam energy distribution (right). The beam profile is shown in grey.

Heating due to Wake Fields

The wake fields computed with both geometry models are then used to estimate the heating power.

Taking an electron located at position s within the beam that travels a length L in the vacuum chamber, the energy loss per meter travelled for this electron is:

$$\delta_w^E(s) = \frac{W_f(s) \cdot L \cdot e}{L} = W_f(s) \cdot e, \tag{7}$$

where e is the charge of the electron. Then after travelling one meter in the vacuum chamber, the energy loss of the entire electron beam is:

$$\Delta E_B^{rw+rs} = \int_0^{l_B} \delta_w^E(s') \frac{f(s')}{e} ds' . \tag{8}$$

Finally, taking into account the repetition rate of the electron beams that pass the undulator lines, the heat generation rate per unit length (with the unit W/m) is calculated according to:

$$\frac{dP^{rw+rs}}{dz} = -\Delta E_B^{rw+ro} \cdot f_{rep}. \tag{9}$$

The total wake field is computed using both round and flat plate models and the heating estimation is summarized in Table 2. The flat plate model predicts slightly higher heat generation rate but is still the favourable geometry choice since it induces less energy variation along the electron beam.

Table 2 Wake Field Induced Heat Generation Rate Per Unit Length

Model	Round Pipe	Flat Plate
dP^{rw+rs}/dz [W/m]	2.0487	2.2722

SYNCHROTRON RADIATION

Synchrotron radiation emitted by relativistic electron beams in the undulators may be absorbed by the chamber walls. The total synchrotron radiation power after passing through a length L_u is calculated with [8]:

$$P^{sr} = e\gamma^2 \frac{\langle I \rangle}{12\pi\varepsilon_0} \left(\frac{2\pi}{\lambda_u}\right)^2 K^2 L_u, \tag{10}$$

where γ is the Lorentz factor, λ_u is the undulator period, K is the undulator parameter and $\langle I \rangle$ is the average current of the electron beams calculated by:

$$\langle I \rangle = Q_B f_{rep}. \tag{11}$$

Q_B is the charge of each electron beam. Assuming conservatively that half the power will be absorbed by the vacuum chamber, the heat generation rate per unit length due to synchrotron radiation is then given by:

$$\frac{dP^{sr}}{dz} = 0.5 \frac{P^{sr}}{L_u}. \tag{12}$$

The typical undulator parameter K values at S[3]FEL ranges from 1 to 5. Considering the case where 15 nm radiation is generated with an undulator period of 0.043 m, the corresponding undulator K value is 5.6034. In this case, the synchrotron radiation related heat generation calculated according to Eq. (10) and Eq. (12) is 0.38537 W/m.

CONCLUSION

In this paper, the heat generation rates in the S[3]FEL undulator vacuum chambers are estimated. The electron beam longitudinal profile in the undulator is obtained from a start-to-end simulation and is used to compute the contributions wake field effects. The synchrotron radiation deposited power is calculated conservatively using an analytical expression. The estimated total heating power is approximately 2.6 W/m and should be easily compensated with the cooling water system.

ACKNOWLEDGEMENTS

The authors thank Wei Wei (IASF) for providing the vacuum chamber geometry shown the vacuum in Fig. 1. This work is supported by the Shenzhen Science and Technology Program (Grant No. RCBS20210609104332002), the Scientific Instrument Developing Project of Chinese Academy of Sciences (Grant No. GJJSTD20190002) and the National Natural Science Foundation of China (22288201).

REFERENCES

[1] X. Wang *et al.*, "Physical design for Shenzhen superconducting soft x-ray free-electron laser (S[3]FEL)", in *Proc. IPAC'23*, Venice, Italy, 2023, paper TUPL043. `https://doi.org/10.18429/JACoW-14th International Particle Accelerator Conference-TUPL043`

[2] K. Bane and G. Stupakov, "Roughness Tolerence Studies for the Undulator Beam Pipe Chamber of LCLS-II", SLAC National Accelerator Laboratory, CA, USA, Rep. LCLS-II-TN-14-06, May 2014. `https://doi.org/10.48550/arXiv.1405.0330`

[3] K. Fujita, "Impedance computation of cryogenic vacuum chambers using boundary element method", *Phys. Rev. Accel. Beams.*, vol. 25, no. 6, p. 64601, June 2014. `https://doi.org/10.1103/PhysRevAccel-Beams.25.064601`

[4] K. Bane and G. Stupakov, "Impedance of a beam tube with small corrugations", in *Proc. Linac2000*, Monterey, CA, USA, Aug. 2000, pp. 92-94.

ISBN: 978-3-95450-265-3 doi:10.18429/JACoW-SAP2023-TUPB033

https://doi.org/10.48550/arXiv.physics/0008205

[5] G. Stupakov and S. Reiche, "Surface roughness wakefield in FEL undulator", in *Proc. FEL2013*, New York, NY, USA, Aug. 2013, pp. 127-131. https://accelconf.web.cern.ch/FEL2013/papers/mopso73.pdf

[6] G. Stupakov, "Surface impedance and synchronous modes", in *AIP Conference Proceedings*, vol. 496, no. 1, pp. 341-350, 1999. https://doi.org/10.1063/1.1301898

[7] H. Henke and O. Napoly, "Wake fields between two parallel resistive plates", in *Proc. EPAC90'*, Nice, France, 1990, pp. 1046-1048. https://accelconf.web.cern.ch/e90/PDF/EPAC1990_1046.PDF

[8] KJ. Kim et al., "Synchrotron radiation and free-electron lasers". Cambridge university press, 2017.